Histol Histopathol (2023) 38: 1043-1053

Histology and Histopathology
From Cell Biology to Tissue Engineering

ORIGINAL ARTICLE Open Access

Induction of lncRNA MALAT1 by hypoxia promotes bone formation by regulating the miR-22-3p/CEBPD axis

Jiang Huang, Hui-liang Shen, Ming-li Feng, Zheng Li, Shuai An and Guang-lei Cao
Department of Orthopedics, Xuanwu Hospital, Capital Medical University, Beijing, China

Summary. Adaptation to hypoxia promotes fracture healing. However, the underlying molecular mechanism remains unknown. Increasing evidence has indicated that long non-coding RNAs (lncRNAs) play crucial roles in several diseases, including fracture healing. In the present study, lncRNA microarray analysis was performed to assess the expression levels of different lncRNAs in MC3T3-E1 cells cultured under hypoxic conditions. A total of 42 lncRNAs exhibited significant differences in their expression, including metastasis associated lung adenocarcinoma transcript 1 (MALAT1), maternally expressed 3, AK046686, AK033442, small nucleolar RNA host gene 2 and distal-less homeobox 1 splice variant 2. Furthermore, overexpression of MALAT1 promoted osteoblast differentiation, alkaline phosphatase (ALP) activity and matrix mineralization of MC3T3-E1 cells, whereas its knockdown diminished hypoxia-induced cell differentiation, ALP activity and matrix mineralization in these cells. Moreover, functional analysis indicated that MALAT1 regulated the mRNA and protein expression levels of CCAAT/enhancer binding protein δ by competitively binding to microRNA-22-3p. Adenoviral-mediated MALAT1 knockdown inhibited fracture healing in a mouse model. Taken together, the results indicated that MALAT1 may serve a role in hypoxia-mediated osteogenesis and bone formation.

Key words: Hypoxia, Metastasis associated lung adenocarcinoma transcript 1, microRNA-22-3p, Differentiation, CCAAT/enhancer binding protein δ

Corresponding Author: Guang-lei Cao, MD, PHD, Department of Orthopedics, Xuanwu Hospital, Capital Medical University, No. 45, Changchun Street, Xicheng District, Beijing, 100053, China. e-mail: gregary111@163.com
www.hh.um.es. DOI: 10.14670/HH-18-569

Introduction

Bone fracture is a common clinical condition and represents an enormous financial burden (Braithwaite et al., 2003; Bishop et al., 2012; Buza and Einhorn, 2016). Bone fracture healing is a series of complex and multi-step processes involving cellular and systemic changes. However, failure of fracture healing usually results in either delayed or impaired healing (Buza and Einhorn, 2016). Previous studies have shown that hypoxic conditions promote fracture healing *in vivo*. However, the exact cellular and molecular mechanisms of fracture healing remain unknown.

The development of high-throughput genome and transcriptome sequencing has led to the identification of long non-coding RNAs (lncRNAs), which are transcribed RNA molecules longer than 200 nucleotides in length with no protein coding capacity (Esteller, 2011; Huarte, 2015; Liu et al., 2019a,b). Accumulating evidence has shown that lncRNAs are involved in a variety of biological processes and that their aberrant expression is implicated in the development of various diseases (Cesana et al., 2011; Esteller, 2011). Recently, several studies have shown that lncRNAs play important roles in fracture healing by mediating osteogenic differentiation. lncRNA-anti-differentiation non-coding RNA has been reported to inhibit osteoblast differentiation by regulating enhancer of zeste homolog 2/runt-related transcription factor 2 (Runx2) expression (Zhu and Xu, 2013). It has also been shown that lncRNA regulator of reprogramming promotes osteogenic differentiation of mesenchymal stem cells by acting as a competing endogenous RNA (ceRNA) of microRNA (miRNA/miR)-138 and miR-145, which target zinc finger E-box binding homeobox 2 to activate the Wnt/β-catenin signaling pathway (Feng et al., 2018). However, the roles of several lncRNAs and the molecular mechanisms associated with osteogenic differentiation and fracture healing remain largely unclear.

To systematically identify the changes in lncRNA expression during osteogenic differentiation, lncRNA profiling was performed to detect differentially expressed lncRNAs in MC3T3-E1 cells in the presence

or absence of hypoxia. Among the differentially expressed lncRNAs, metastasis associated lung adenocarcinoma transcript 1 (MALAT1) expression was upregulated and, therefore, this lncRNA was selected for further experiments. The findings suggested that the upregulation of MALAT1 led to osteogenic differentiation, without affecting cell proliferation and apoptosis. Further studies demonstrated that lncRNA MALAT1 was able to directly bind to miR-22-3p and act as a miRNA sponge to regulate CCAAT/enhancer binding protein δ (CEBPD) expression.

Materials and methods

Cell culture and treatment

The mouse osteoblastic MC3T3-E1 cell line was purchased from The Cell Bank of Type Culture Collection of The Chinese Academy of Sciences. MC3T3-E1 cells were cultured in a-MEM (HyClone; Cytiva) supplemented with 10% FBS (Invitrogen; Thermo Fisher Scientific, Inc.), 100 IU/ml penicillin (Invitrogen; Thermo Fisher Scientific, Inc.) and 100 mg/ml streptomycin (Invitrogen; Thermo Fisher Scientific, Inc.). The cells were incubated in a 5% CO_2 humidified atmosphere at 37°C. Hypoxia experiments were performed in a hypoxia chamber at 5% O_2 in a 5% CO_2 humidified environment at 37°C for 24h. *In vitro* osteoblast differentiation of MC3T3-E1 cells was performed using osteogenic induction medium containing standard growth medium supplemented with 50 mg/l ascorbic acid, 10 mmol/l β-glycerophosphate and 10 nmol/l dexamethasone (Sigma-Aldrich; Merck KGaA) every 2 days.

lncRNA profiling and data analysis

MC3T3-E1 cells were exposed to hypoxic conditions for 24h and lncRNA microarray analysis was performed using mouse lncRNA Microarray V2.0 (KangChen Bio-tech, Shanghai, China). RNA extraction from cells was performed according to the manufacturer's protocol. The differentially expressed lncRNAs were selected based on the threshold values of >2.0 or <-2.0 and a Benjamini-Hochberg-corrected P value was set at <0.05. Quantile normalization and raw data were analyzed using GeneSpring GX v11.5 software package (Agilent Technologies, Inc.). Pathway analysis for differentially expressed lncRNAs was performed using the Kyoto Encyclopedia of Genes and Genomes (KEGG; http://www.genome.jp/kegg) database.

Tibial fracture model and treatment

C57BL/6 mice (age, 10 weeks) were purchased from Shanghai Laboratory Animals Center. The mice were housed in sterilized cages at the Experimental Animal Center of Capital Medical University. All animal care and experimental procedures were performed in accordance to the National Institute of Health guidelines for Care and Use of Laboratory Animals and were approved by the Capital Medical University Committee of Animal Resources (approval no. 201608RD). The mice (8/each group) were anesthetized with pentobarbital sodium (30 mg/kg) by intraperitoneal injection. Subsequently, they were sacrificed by cervical dislocation on days 21, 28 and 42. A closed tibial fracture model was established using a Bose Electroforce 3200 mechanical instrument (Eden Prairie) in 12-week-old male BALB/c mice (n= 8/group) as determined by our previous study (Huang et al., 2015a,b).

Reverse transcription-quantitative PCR (RT-qPCR)

Total RNA was extracted from cell and tissue samples using TRIzol® reagent (Invitrogen; Thermo Fisher Scientific, Inc.) as previously described (Huang et al., 2015a,b). qPCR was performed using Fast SYBR™ Green Master Mix (Thermo Fisher Scientific, Inc.) with specific primers according to the manufacturer's specifications. The primers used were as follows: Alkaline phosphatase (ALP) forward, 5'-TGGCTCTGC CTTTATTCCCTAGT-3' and reverse, 5'-AAATAAGGT GCTTTGGGAATCTGT-3'; Runx2 forward, 5'-GCCGGGAATGATGAGAACTA-3' and reverse, 5'-GGTGAAACTCTTGCCTCGTC-3'; osteocalcin forward, 5'-GCCATCACCCTGTCTCCTAA-3' and reverse, 5'-GCTGTGGAGAAGACACACGA-3'; GAPDH forward, 5'-CATCCCAGAGCTGAACG-3' and reverse, 5'-CTGGTCCTCAGTGTAGCC-3'; miR-22-3p forward, 5'-AAGCTGCCAGTTGAAGAACTGT-3' and reverse, 5'-ACAGTTCTTCAACTGGCAGCTT-3'; and U6 forward, 5'-GGTCGGGCAGGAAAGAGGGC-3' and reverse, 5'-GCTAATCTTCTCTGTATCGTTCC-3'. The relative gene expression was analyzed using the $2^{-\Delta\Delta Cq}$ method (Livak and Schmittgen, 2001). U6 and β-actin were used to normalize the target gene expression.

Adenoviral construction and infection

To establish adenoviruses encoding MALAT1, its full-length sequence was amplified by RT-qPCR and subsequently cloned into a pShuttle-CMV vector (Hanbio Biotechnology Co., Ltd.). The procedures for recombinant adenoviral production, purification and titration were performed as described in a previous study (Singpiel et al., 2018). Adenoviruses containing MALAT1 were locally injected into the distraction gap monitored by X-ray on the second day post-surgery. At the end of the experimental period, the mice were sacrificed, and the tibial specimens were harvested for further analysis.

Cell viability assay and apoptosis

To determine the effects of MALAT1 on MC3T3-E1 cells, cell viability and apoptosis were measured as

described in a previous study (Huang et al., 2016). MC3T3-E1 cells were transfected with negative control (NC) or MALAT1 and seeded into 96-well plates. The cells were cultured for 24, 48 and 72h. A total of 10 µl Cell Counting Kit-8 reagent (Dojindo Molecular Technologies, Inc.) was added to each well and the optical density was measured at 450 nm using a microplate reader (Bio-Rad Laboratories, Inc.). Cell apoptosis was determined using a Annexin V-FITC Apoptosis Detection kit I (BD Biosciences). The apoptotic rate was analyzed using FlowJo software (version 10.0; FlowJo LLC). The apoptotic rate (%) was calculated as follows: (Cell number in Q4/cell number in all quadrants) x100, with cells in Q3 representing early apoptotic cells.

Dual-luciferase reporter assay

The full-length cDNA of MALAT1 and the wild type 3′-untranslated region (UTR) of the CEBPD gene containing the putative miR-22-3p binding sites were amplified by RT-qPCR and inserted into the pMIR-REPORT™ vector (Ambion; Thermo Fisher Scientific, Inc.). The mutant (MUT) MALAT1 and CEBPD 3′-UTRs were generated using the QuikChange Site-Directed Mutagenesis kit (Agilent Technologies, Inc.). 293T cells were co-transfected with miR-NC or miR-22-3p mimics using Lipofectamine® 3000 reagent (Invitrogen; Thermo Fisher Scientific, Inc.). Following 24h of cell culture, the dual-luciferase reporter assay was performed as described in a previous study (Huang et al., 2016).

Micro-CT scan and analysis

Mouse tibiae were harvested, washed with PBS and fixed in 70% ethanol. The structure and mineralization of the tibia fracture callus were scanned using a microtomographic imaging system (µCT 40, Scanco Medical). Callus bone mineral density (BMD) and bone volume/tissue volume (BV/TV) were determined at the indicated time points.

Alizarin Red S staining and alkaline phosphatase activity assay

The Alizarin Red S staining and ALP activity assays were performed as described in a previous study (Huang et al., 2016).

Immunohistochemical (IHC) analysis

Tibias were fixed with 4% paraformaldehyde for 24h and decalcified for 6 weeks in 15% EDTA at room temperature. IHC analysis was performed using a standard histological staining protocol as described previously (Huang et al., 2015a,b). Staining was assessed by semi-quantitative analysis using an Olympus BX51 microscope (Olympus Corporation). An Olympus DP71 camera and DP Manager (Olympus Corporation) imaging software were used for analysis.

RNA pull-down assay

MALAT1 fragments were obtained using Riboprobe® *in vitro* Transcription Systems (Promega Corporation). The fragments were labeled with biotin using the Biotin 3' End DNA Labeling kit (Beyotime Institute of Biotechnology). The RNA, which was bound, was harvested by magnetic beads and analyzed by RT-qPCR.

Western blotting

Total protein was extracted from cells and fracture tissues using RIPA lysis buffer (Cell Signaling Technology, Inc.) supplemented with complete protease inhibitors (Roche Diagnostics). The standard protocol was performed to detect the protein expression using 10% SDS-PAGE. The membranes were incubated with antibodies against CEBPD (cat. no. ab65081; 1:1,000; Abcam), ALP (cat. no. ab84401; 1:1,000; Abcam), Runx2 (cat. no. H00000860-M04; 1:500; Abnova), osteocalcin (cat. no. ab13418; 1:1,000; Abcam) and mouse monoclonal β-actin (cat. no. sc-47778; 1:5,000; Santa Cruz Biotechnology, Inc.). GAPDH was used as a loading control.

Statistical analysis

All data are presented as the mean ± SD and all experiments were carried out in triplicates and repeated three times at least. Statistical differences were assessed using a Student's t-test or one-way ANOVA followed by a Tukey's test. lncRNA profiling and data analysis were performed using GeneSpring GX software v13.0 (Agilent Technologies, Inc.). Statistical analysis was conducted using SPSS 16.0 software (SPSS, Inc.). $P<0.05$ was considered to indicate a statistically significant difference.

Results

Aberrant expression of MALAT1 in hypoxia-induced MC3T3-E1 cells

In order to identify the lncRNAs involved in fracture healing, murine lncRNA microarray analysis was performed in MC3T3-E1 cells cultured under hypoxic conditions for 24h and in their parental cells. An unsupervised analysis using conventional hierarchical agglomerative clustering was performed to identify the dysregulated lncRNAs and mRNAs whose average change in expression levels varied ≥2-fold (Fig. 1A). There were 24 up-regulated genes and 18 down-regulated genes that were enrolled for further investigation (Fig. 1B). The expression levels of the top up- and downregulated lncRNAs were consistent with

those reported by the microarray data as determined by RT-qPCR (Fig. 1C,D). In addition, KEGG pathway analysis identified the top seven most enriched pathways corresponding to upregulated mRNAs, including the 'HIF-1 signaling pathway', 'metabolic pathways' and the 'VEGF signaling pathway' (Fig. 1E). Furthermore, the top eight enriched pathways corresponding to downregulated mRNA expression levels were also identified, such as those involved in 'fatty acid biosynthesis', 'arachidonic acid metabolism' and 'one carbon pool by folate' (Fig. 1F). Furthermore, MALAT1 levels were increased in MC3T3-E1 cells cultured under hypoxic conditions (Fig. 2A). MALAT1 expression was increased in HUVECs exposed to 1% O_2 as determined by RNA-sequencing and was induced in a mouse model of hindlimb ischemia (Michalik et al., 2014; Voellenkle et al., 2016). MALAT1 expression was transcriptionally activated by hypoxia-inducible factor 1-α and was upregulated in renal ischemia-reperfusion injury models (Kölling et al., 2018). MALAT1 was also reported to play an important role in cardiovascular disease (Liu et al., 2020; Wang et al., 2019). MALAT1 was selected for investigation in subsequent experiments due to its function, which was reported in previous studies. The expression levels of MALAT1 were increased following fracture compared with those noted in the normal bone tissues (Fig. 2B). In addition, MALAT1 expression was significantly increased during osteogenic induction (Fig. 2C). A positive correlation between the expression levels of MALAT1 and ALP activity was noted in MC3T3-E1 cells during osteogenic induction (Fig. 2D). These results indicated that MALAT1 may be involved in

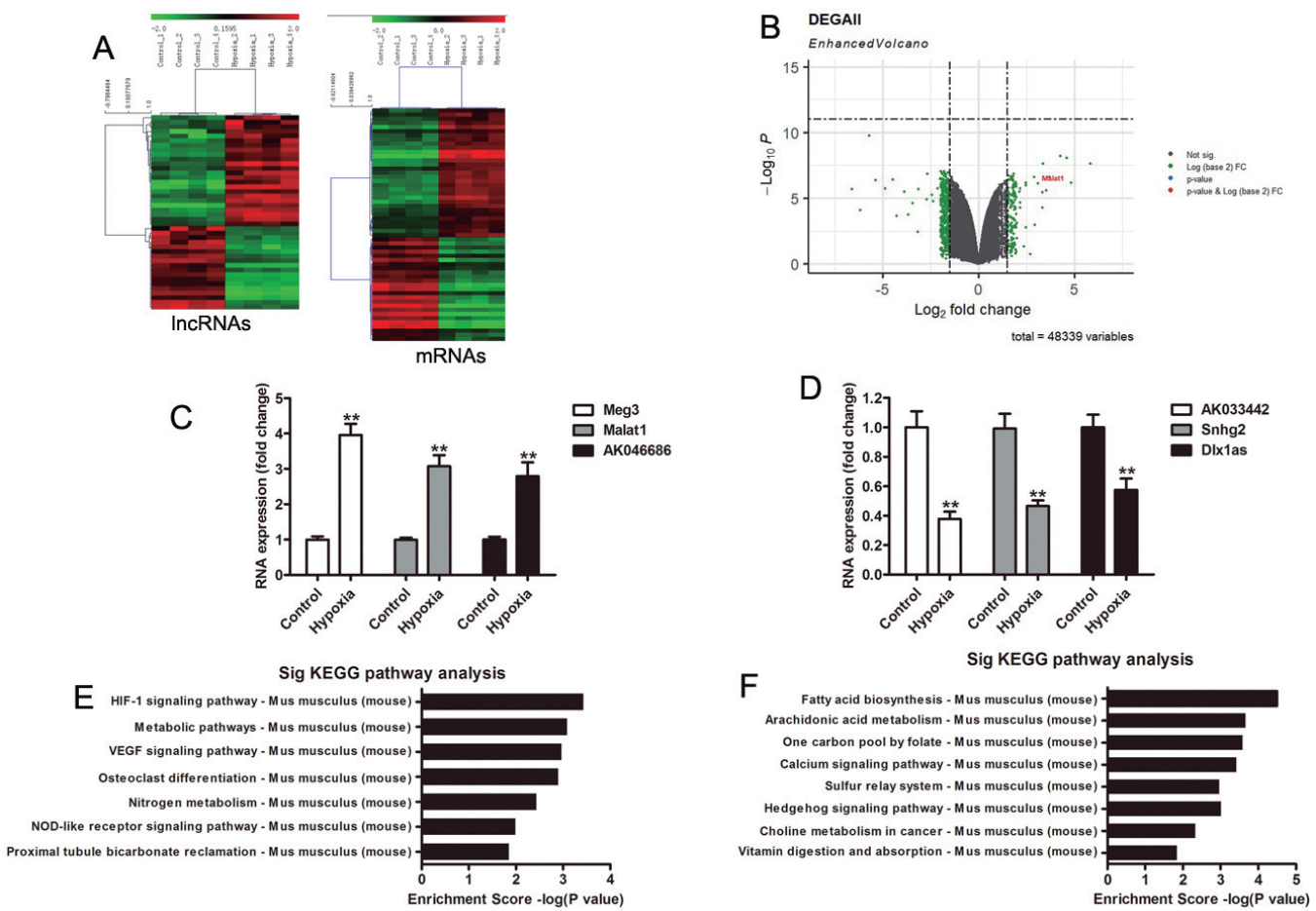

Fig. 1. Expression levels of lncRNA MALAT1 are significantly increased in MC3T3-E1 cells following induction of hypoxia. **A.** Heat map indicating hierarchical clustering of differentially expressed lncRNAs and mRNAs in MC3T3-E1 cells in the absence or presence of hypoxia. Relative high (red) or low (green) expression as indicated. **B.** Volcano map of gene chip. Validation of upregulation **(C)** and downregulation **(D)** of lncRNA expression by reverse transcription-quantitative PCR in MC3T3E cells with or without hypoxia. **E.** Kyoto Encyclopedia of Genes and Genomes pathway analysis indicates the top seven most enriched pathways based on the upregulation **(E)** and downregulation **(F)** of mRNA levels under hypoxic conditions. **P<0.01. lncRNA, long non-coding RNA; MALAT1, metastasis associated lung adenocarcinoma transcript 1.

fracture healing.

Effects of MALAT1 on MC3T3-E1 cell differentiation and ALP activity

To evaluate the effects of MALAT1 on specific cellular processes, MC3T3-E1 cells were transfected with adenoviral vectors containing MALAT1. MALAT1 levels were significantly increased in MC3T3-E1 cells transfected with MALAT1 vectors compared with those noted in the NC cells, as determined by RT-qPCR analysis (Fig. 3A). Subsequently, the ability of MALAT1 to induce differentiation of MC3T3-E1 cells was assessed. The results indicated that overexpression of MALAT1 promoted osteogenic differentiation of MC3T3-E1 cells following induction of cells in osteogenic media for 21 days, as determined by Alizarin Red staining (Fig. 3B). Significantly higher mRNA levels of several osteogenic marker genes (ALP, Runx2 and osteocalcin) were observed in MC3T3-E1 cells transfected with MALAT1 vector compared with those noted in the NC cells (Fig. 3C). The ALP activity levels in the MALAT1-overexpressing cells were also significantly increased compared with those of the NC cells (Fig. 3D). However, no significant changes were noted in cell viability and the levels of apoptosis of MALAT1-overexpressing cells following their induction in osteogenic media at the indicated time periods (Fig. 3E,F). The protein levels of ALP, Runx2 and osteocalcin were increased in MC3T3-E1 cells transfected with MALAT1 vector compared with those noted in the control cells (Fig. 3G). The results were consistent with those noted for the mRNA levels of these markers, suggesting that the early upregulation of MALAT1 expression may facilitate fracture healing by inducing the expression of ALP, Runx2 and osteocalcin.

MALAT1 acts as a sponge of miR-22-3p in MC3T3-E1 cells

It has been shown that lncRNAs regulate the expression levels of various critical genes by competitively suppressing the expression of specific miRNAs (Cesana et al., 2011). To fully understand the mechanism associated with cell differentiation following upregulation of MALAT1 expression, bioinformatics software was used to predict potential miRNAs, which may influence osteogenic differentiation. Bioinformatics analysis (http://starbase.sysu.edu.cn/index.php) indicated that MALAT1 may act as a sponge of miR-22-3p, causing the downregulation of its expression during osteoblast differentiation (Fig. 4A) (Choi et al., 2017). A dual-luciferase reporter assay was performed to validate the binding of miR-22-3p to MALAT1 and the results indicated that the luciferase activity was markedly reduced in MALAT1-wild-type, but not in MALAT1-MUT cells (Fig. 4B). Since miR-22-3p might directly bind to MALAT1, the overexpression of MALAT1 was hypothesized to decrease its expression levels. As expected, miR-22-3p expression was significantly decreased in MC3T3-E1 cells transfected with MALAT1 vector (Fig. 4C). In addition, binding of miR-22-3p to MALAT1 was further confirmed using RNA pull-down assays and the results indicated that the enrichment of miR-22-3p was significantly increased in MALAT1-overexpressing cells compared with that of the NC cells

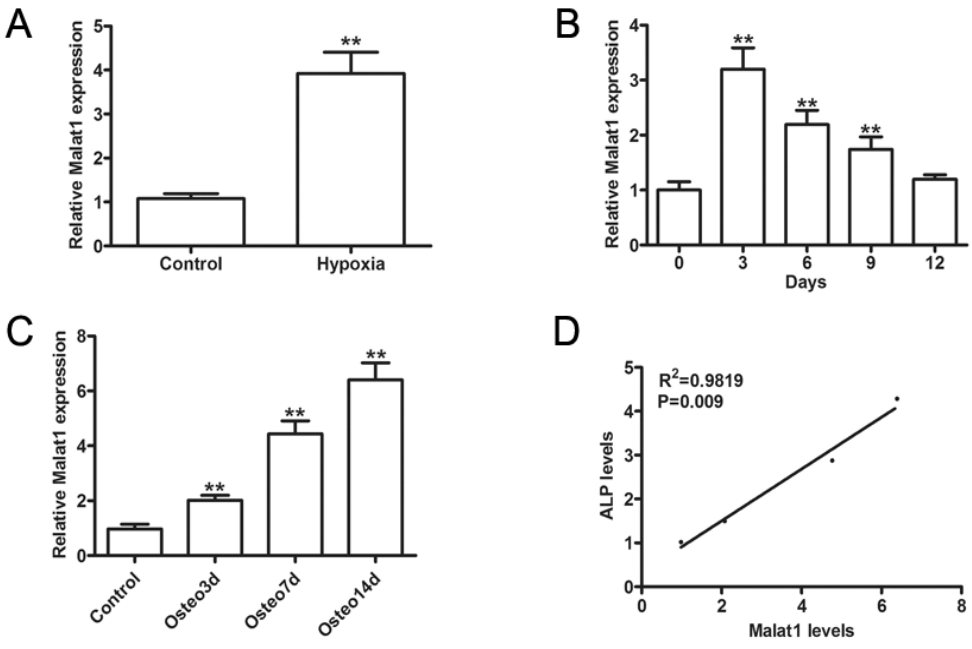

Fig. 2. MALAT1 expression is induced following hypoxia. **A.** MALAT1 expression levels were analyzed in MC3T3-E1 cells with or without hypoxia using reverse transcription-quantitative PCR analysis. **B.** Expression levels of MALAT1 in bone tissues were evaluated at the indicated time periods. **C.** Expression levels of MALAT1 were determined following osteogenic induction. **D.** Correlation analysis between MALAT1 levels and ALP activity in MC3T3E cells at the indicated time periods following osteogenic induction. **P<0.01. MALAT1, metastasis associated lung adenocarcinoma transcript 1; ALP, alkaline phosphatase.

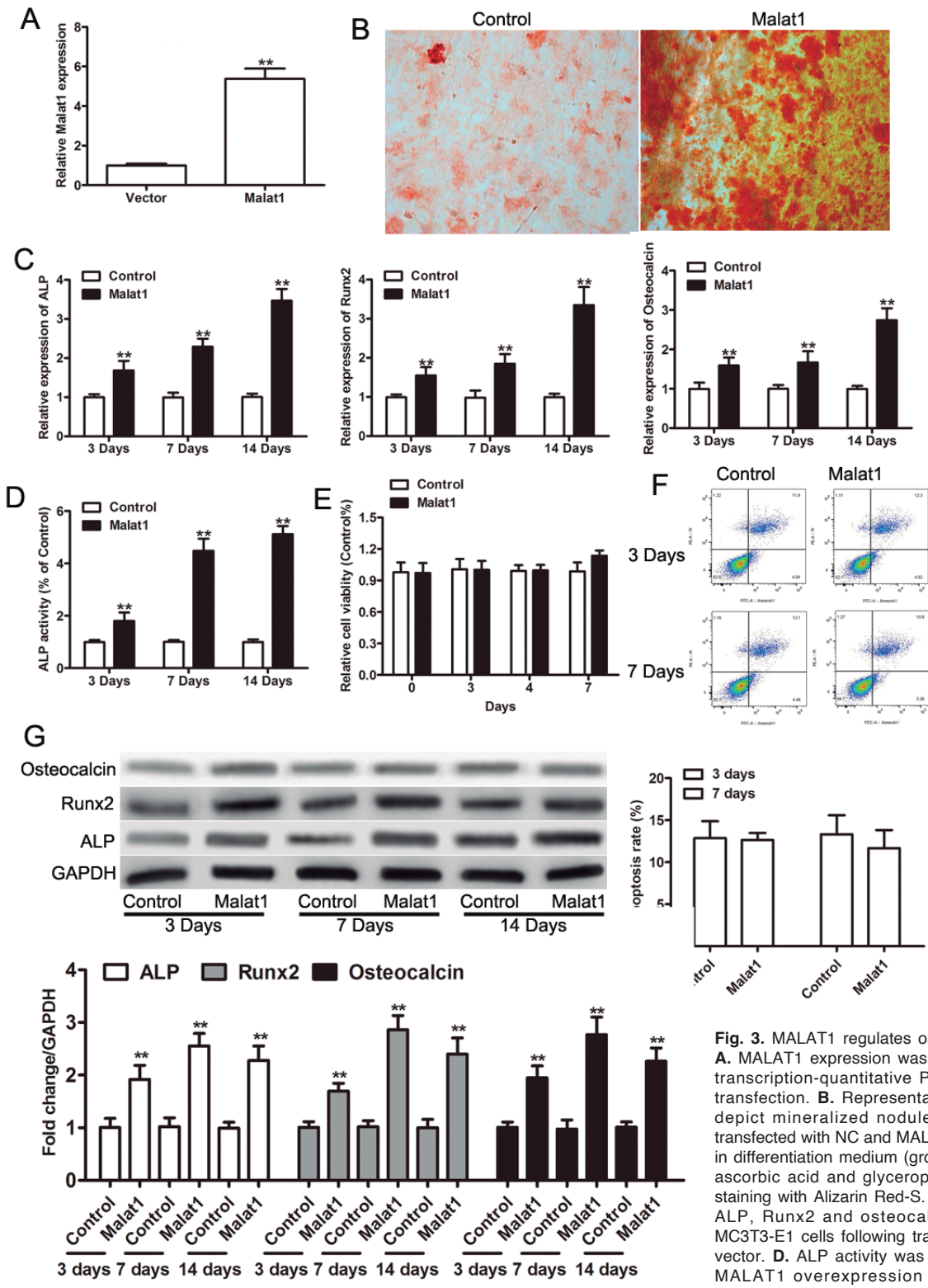

Fig. 3. MALAT1 regulates osteoblast differentiation. **A.** MALAT1 expression was determined by reverse transcription-quantitative PCR analysis following transfection. **B.** Representative photomicrographs depict mineralized nodules in MC3T3-E1 cells transfected with NC and MALAT1 vectors for 14 days in differentiation medium (growth medium containing ascorbic acid and glycerophosphate) followed by staining with Alizarin Red-S. **C.** Expression levels of ALP, Runx2 and osteocalcin were detected in MC3T3-E1 cells following transfection with MALAT1 vector. **D.** ALP activity was markedly increased by MALAT1 overexpression following osteogenic induction. Cell viability **(E)** and apoptosis **(F)** were not altered following MALAT1 overexpression. **G.** Western blot analysis was performed to assess the expression levels of ALP, Runx2, and osteocalcin at 3, 7 and 14 days following MALAT1 overexpression. **P<0.01. Malat1, metastasis associated lung adenocarcinoma transcript 1; ALP, alkaline phosphatase; Runx2, runt-related transcription factor 2; NC, negative control.

(Fig. 4D). These data provided strong evidence to suggest that MALAT1 acted as a sponge for miR-22-3p by direct binding.

miR-22-3p is involved in MALAT1-mediated CEBPD expression

It has been reported that miR-22 negatively regulates bone formation by targeting osteocalcin (Choi et al., 2017). Subsequently, the genes that were potentially regulated by miR-22-3p were investigated in order to characterize the effects of MALAT1. The miRNA target prediction database was used to predict the targets of miR-22-3p and CEBPD was identified as one of its targets (Fig. 5A). The results of the dual-luciferase reporter assay indicated that the luciferase activity was significantly decreased following co-transfection of the cells with miR-22-3p mimic and a luciferase reporter construct containing the wild-type CEBPD 3′-UTR, whereas mutation of the binding seed site abolished miR-22-3p-mediated luciferase activities (Fig. 5B). Moreover, the endogenous mRNA and protein levels of CEBPD were significantly decreased in MC3T3-E1 cells transfected with miR-22-3p mimic (Fig. 5C,D). In the present study, it was hypothesized that the miR-22-3p/CEBPD axis could interact with MALAT1 via a ceRNA-dependent mechanism. To confirm the positive association between the expression levels of MALAT1 and CEBPD, the association between MALAT1 and CEBPD expression levels was assessed. As expected, the mRNA and protein expression levels of CEBPD were significantly decreased in MC3T3-E1 cells transfected with MALAT1 vector compared with those of the NC cells (Fig. 5E,F). To determine whether miR-22-3p played a crucial role in the association between MALAT1 and CEBPD, MC3T3-E1 cells were co-transfected with MALAT1 vector and miR-22-3p mimic. Overexpression of MALAT1 increased the expression levels of CEBPD and of the osteogenic marker genes, whereas the overexpression of miR-22-3p effectively abrogated these effects. Collectively, these results indicated that CEBPD was the functional target protein of miR-22-3p and that MALAT1 was involved in the post-transcriptional regulation of CEBPD by sponging miR-22-3p.

Local injection of MALAT1 enhances bone formation in an animal model

Since MALAT1 can promote osteogenesis *in vitro*, its role in bone formation was examined *in vivo*. A total of 10 µl recombinant adenovirus ($1x10^{12}$ pfu/ml) was locally injected into the distraction gap following fracture. At 4 weeks following fracture, micro-CT analysis indicated a higher amount of bony callus at the fracture site in the MALAT1-treated mice than in the control group (Fig. 6A). Higher BV/TV and BMD were also observed in the MALAT1-treated mice (Fig. 6B,C). As expected, the expression levels of MALAT1 were significantly increased in the MALAT1-treated mice (Fig. 6D). Histological analysis confirmed that MALAT1 induced expression of osteogenic markers (ALP and osteocalcin) and CEBPD *in vivo* during bone regeneration and remodeling (Fig. 6E).

Discussion

An increasing number of studies have shown that lncRNAs play key roles in numerous biological processes. Further studies have indicated that lncRNAs can regulate the osteogenic differentiation of mesenchymal stem cells, suggesting their potential functions in the progression of fracture healing (Huang et al., 2015a,b; Feng et al., 2018; Peng et al., 2018).

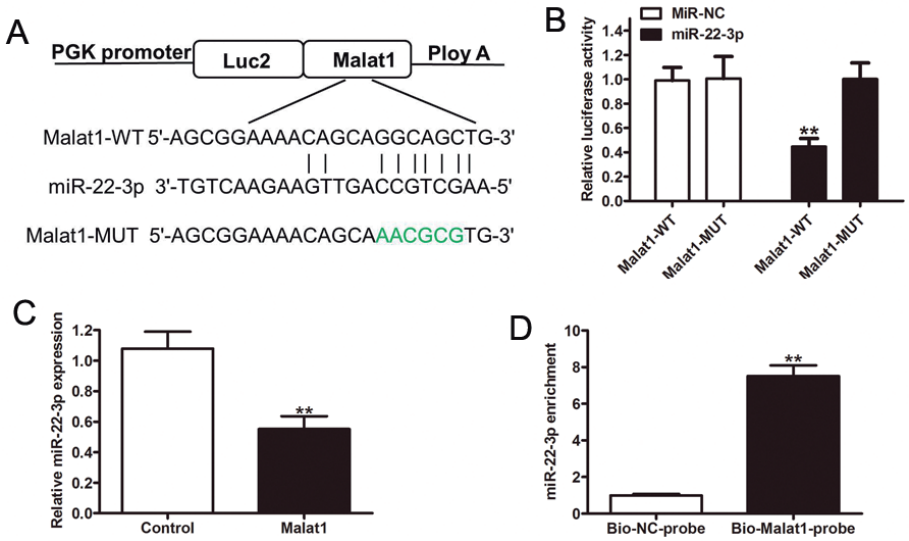

Fig. 4. MALAT1 acts as a sponge of miR-22-3p in MC3T3-E1 cells. **A.** Binding sites between the wild-type MALAT1 and/or the MUT MALAT1 and miR-22-3p were predicted with online bioinformatics analysis (http://starbase.sysu.edu.cn/mirLncRNA.php). **B.** Dual-luciferase reporter assays were used to confirm the binding between MALAT1 and miR-22-3p in MC3T3-E1 cells. **C.** Endogenous expression of miR-22-3p in MC3T3-E1 cells transfected with control or MALAT1 vectors. **D.** Detection of miR-22-3p expression using reverse transcription-quantitative PCR analysis in samples pulled down by biotinylated MALAT1 and NC probes. **P<0.01. Malat1, metastasis associated lung adenocarcinoma transcript 1; miR-22-3p; microRNA-22-3p; MUT, mutant; NC, negative control.

Previous studies have suggested that hypoxia adaptation improves fracture healing by stimulating VEGF and placental growth factor expression (Maes et al., 2006, 2012; Potente et al., 2011). However, to the best of our knowledge, little is known regarding the association of lncRNAs with osteoblastic cell differentiation. In the present study, the lncRNA profile was used to identify potential lncRNAs associated with bone differentiation and fracture healing. Elevated expression of MALAT1 was observed in both trabecular bones and MC3T3-E1 cells treated with hypoxia, indicating that MALAT1 may play an important role during the progression of fracture repair. *In vitro* assays demonstrated that overexpression of MALAT1 enhanced osteoblastic cell differentiation, while it did not affect cell proliferation and apoptosis. *In vivo* experiments further confirmed that overexpression of MALAT1 promoted fracture repair and bone remodeling under pathological conditions.

Several studies have shown that MALAT1 can regulate cell differentiation. It has been shown that MALAT1 regulates myoblast differentiation by modulating the expression of serum response factor via regulating miR-133 as a ceRNA (Han et al., 2015). Recent reports indicated that MALAT1 promoted osteoblast differentiation of human aortic valve interstitial cells by sponging miR-204 to regulate Smad4 expression (Xiao et al., 2017). MALAT1 has been reported to target miR-22-3p to take part in various pathological processes such as tumor growth and inflammation (Chen et al., 2020; Li et al., 2020). In the

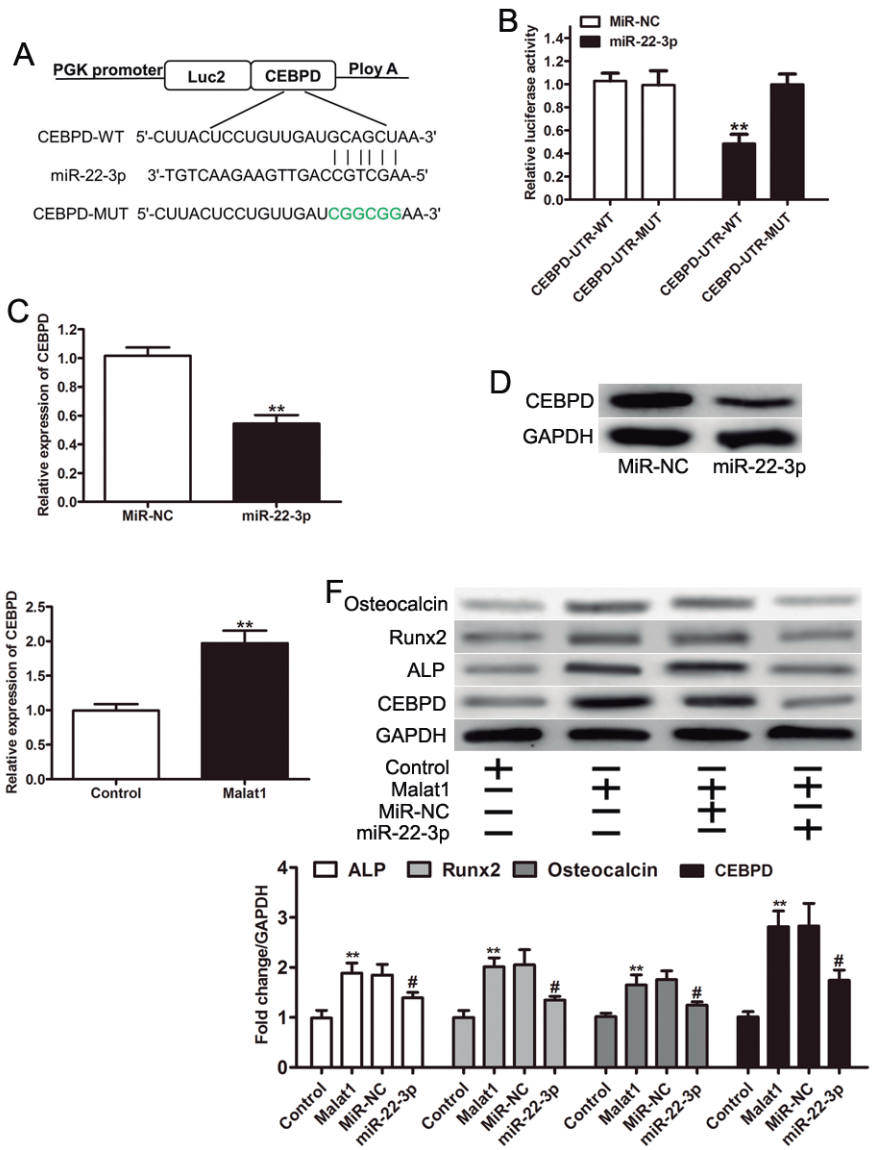

Fig. 5. CEBPD is a direct target of miR-22-3p in MC3T3-E1 cells. **A.** Putative and mutant binding sites in the 3′-UTR of CEBPD and miR-22-3p were predicted using bioinformatics analysis. **B.** miR-22-3p overexpression significantly suppressed the luciferase activity of CEBPD-WT, while co-transfection of MC3T3-E1 cells with miR-22-3p and CEBPD-MUT exhibited no apparent change. Relative mRNA **(C)** and protein **(D)** expression levels of CEBPD in MC3T3-E1 cells transfected with miRNA NC or miR-22-3p mimics were evaluated using reverse transcription-quantitative PCR and western blotting, respectively. **E.** mRNA expression levels of CEBPD were examined in MC3T3-E1 cells transfected with control or MALAT1 vectors. **F.** Expression levels of the CEBPD protein were determined in MC3T3-E1 cells transfected with NC, MALAT1, MALAT1 + miRNA NC, or MALAT1 + miR-22-3p. **P<0.01. CEBPD, CCAAT/enhancer binding protein δ; miR-22-3p, microRNA-22-3p; 3′-UTR, 3′-untranslated region; WT, wild-type; MUT, mutant; NC, negative control; MALAT1; metastasis associated lung adenocarcinoma transcript 1.

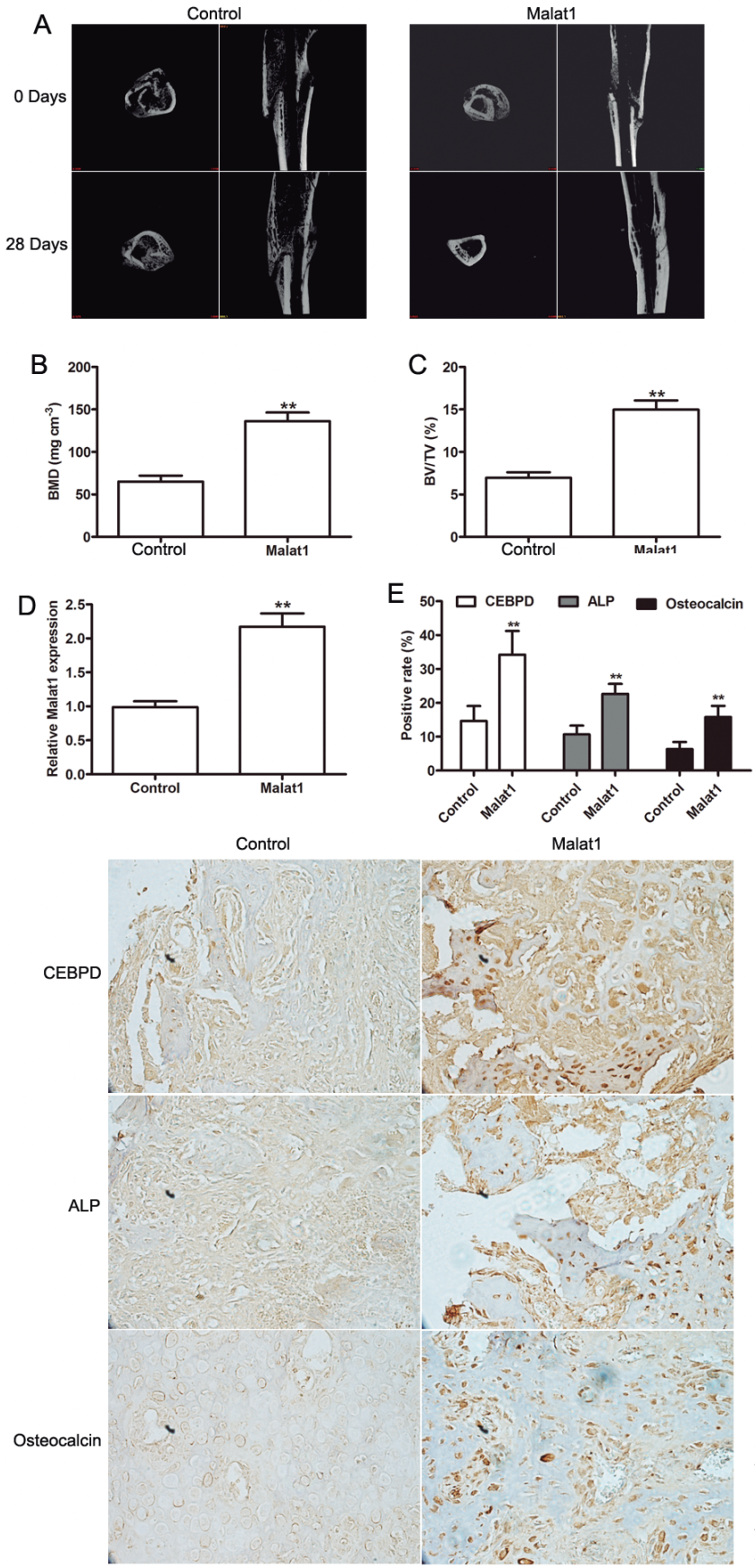

Fig. 6. Bone tissue regeneration is accelerated by local injection of MALAT1 in an animal model. **A.** Representative images indicating bone healing in tibia sites. The images were processed by micro-CT reconstruction. BMD **(B)** and BV/TV **(C)** (%) were increased in callus tissues on the 28th day following surgery in mice transfected with MALAT1. **D.** Immunohistochemical staining was used to assess the expression levels of CEBPD, ALP and osteocalcin following MALAT1 overexpression *in vivo*. **P<0.01. BMD, bone mineral density; BV/TV, bone volume; MALAT1; metastasis associated lung adenocarcinoma transcript 1; CEBPD, CCAAT/enhancer binding protein δ; ALP, alkaline phosphatase.

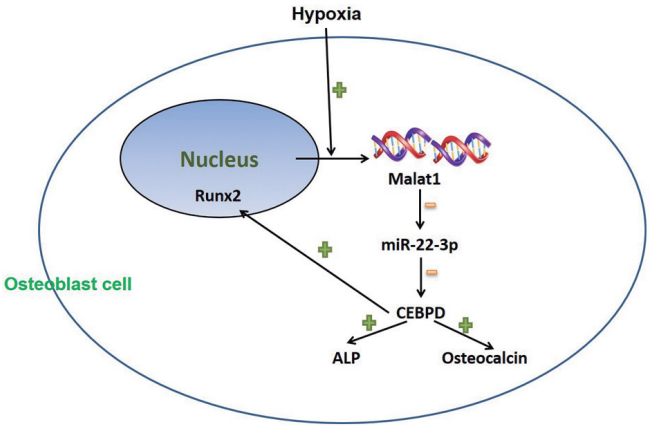

Fig. 7. A schematic diagram that depicts the role of MALAT1 in fracture healing. The expression levels of MALAT1 were induced in the presence of hypoxia. Increased MALAT1 expression causes binding to miR-22-3p, which results in its degradation and the upregulation of CEBPD expression. CEBPD promotes osteogenic differentiation via increased expression of ALP, osteocalcin and Runx2. Malat1; metastasis associated lung adenocarcinoma transcript 1; miR-22-3p; microRNA-22-3p; CEBPD, CCAAT/enhancer binding protein δ; ALP, alkaline phosphatase; Runx2, Runt-related transcription factor 2.

present study, MALAT1 expression was increased following induction of hypoxia in osteoblastic cells. Further *in vitro* studies demonstrated that overexpression of MALAT1 promoted osteoblast differentiation of MC3T3-E1 cells, which was accompanied by upregulation of the expression levels of specific osteogenic markers (ALP, Runx2 and osteocalcin). This finding was consistent with those reported by previous studies. MALAT1 expression is frequently upregulated in human cancers and it has been shown that this lncRNA functions as an oncogene by promoting proliferation and apoptosis (Xie et al., 2017; Xiong et al., 2018). However, the changes in proliferation and apoptosis were not observed following overexpression of MALAT1 in MC3T3-E1 cells. Subsequent *in vivo* experiments confirmed that overexpression of MALAT1 promoted fracture repair. The expression levels of ALP and osteocalcin were significantly increased in mice treated with recombinant adenovirus carrying MALAT1.

Emerging evidence has revealed that lncRNAs act as a ceRNA of miRNAs to regulate gene function expression (Cesana et al., 2011; Liu et al., 2019a,b). In the present study, it was shown that MALAT1 functioned as a ceRNA for miR-22-3p, which has been reported to be involved in osteoblast differentiation *in vivo* (Choi et al., 2017). The direct miR-22-3p/MALAT1 interaction was confirmed by the RNA pull-down and dual-luciferase reporter assays. CEBPD is a member of the leucine-zipper transcription factor family, which participates in several physiological processes. It is a transcription factor that responds to various external stimuli, including the proinflammatory cytokines IL-1β and TNFα and stress and growth factors (Jiang et al., 2015; Li et al., 2017; Banerjee et al., 2019). It has been shown that the expression of CEBPD is associated with adipocyte differentiation and activated osteocalcin gene transcription and synergize with Runx2 at the C/EBP element to regulate bone-specific expression (Kurebayashi et al., 2001; Gutierrez et al., 2002). In the current study, the interaction between miR-22-3p and CEBPD was associated with osteogenic differentiation. The current results provided evidence of MALAT1 acting as a ceRNA for miR-22-3p to regulate CEBPD expression.

In conclusion, the findings of the present study revealed that MALAT1 expression was increased under hypoxia and that its overexpression promoted osteoclast differentiation by acting as a ceRNA of miR-22-3p to regulate CEBPD expression (Fig. 7). The findings suggest a promising therapeutic strategy to facilitate osteogenic differentiation and fracture healing. Notably, MALAT1 expression has been reported to be increased in several cancer types. Therefore, the extension of the present findings into clinical applications requires further investigation.

Ethical Approval. All animal care and experimental procedures were performed in adherence to the National Institute of Health guidelines for Care and Use of Laboratory Animals and were approved the Capital Medical University Committee of Animal Resources. (Permission No: 201608RD).

Author Contribution. Jiang Huang, Shi-bao Lu and Ming-li Feng carried out the assays and clinical consultation. Zheng Li and Shuai An carried out laboratory tests and performed the statistical analysis. Hui-liang Shen and Guang-lei Cao conceived the study, participated in its design and coordination, and drafted the manuscript.

Conflicts of interests. All authors declare that they have no conflicts of interest in this work.

References

Banerjee S., Fu Q., Shah S.K., Melnyk S.B., Sterneck E., Hauer-Jensen M. and Pawar S.A. (2019). C/EBPδ protects from radiation-induced intestinal injury and sepsis by suppression of inflammatory and nitrosative stress. Sci. Rep. 9, 13953.

Bishop J.A., Palanca A.A., Bellino M.J. and Lowenberg D.W. (2012). Assessment of compromised fracture healing. J. Am. Acad. Orthop. Surg. 20, 273-282.

Braithwaite R.S. Col N.F. and Wong J.B. (2003). Estimating hip fracture morbidity, mortality and costs. J. Am. Geriatr. Soc. 51, 364-370.

Buza 3rd J.R. and Einhorn T. (2016). Bone healing in 2016. Clin. Cases Miner. Bone Metab. 13, 101-105.

Cesana M., Cacchiarelli D., Legnini I., Santini T., Sthandier O., Chinappi M., Tramontano A. and Bozzoni I. (2011). A long noncoding RNA controls muscle differentiation by functioning as a competing endogenous RNA. Cell 147, 358-369.

Chen F., Zhong Z., Tan H.Y., Guo W., Zhang C., Cheng C.S., Wang N., Ren J. and Feng Y. (2020). Suppression of lncRNA MALAT1 by betulinic acid inhibits hepatocellular carcinoma progression by targeting IAPs via miR-22-3p. Clin. Transl. Med. 10, e190.

Choi Y.J., Jeong S., Yoon K.A., Sung H.J., Cho H.S., Kim D.W. and Cho J.Y. (2017). Deficiency of DGCR8 increases bone formation through downregulation of miR-22 expression. Bone 103, 287-294.

Esteller M. (2011). Non-coding RNAs in human disease. Nat. Rev. Genet. 12 861-874.

Feng L., Shi L., Lu Y.F., Wang B., Tang T., Fu W.M., He W., Li G. and Zhang J.F. (2018). Linc-ROR promotes ostogenic differentiation of mesenchymal stem cells by functioning as a competing endogenous RNA for miR-138 and miR-145. Mol. Ther. Nucleic Acids 11, 345-353.

Gutierrez S., Javed A., Tennant D.K., van Rees M., Montecino M., Stein G.S., Stein J.L. and Lian J.B. (2002). CCAAT/enhancer-binding proteins (C/EBP) beta and delta activate osteocalcin gene transcription and synergize with Runx2 at the C/EBP element to regulate bone-specific expression. J. Biol. Chem. 277, 1316-1323.

Han X., Yang F., Cao H. and Liang Z. (2015). Malat1 regulates serum response factor through miR-133 as a competing endogenous RNA in myogenesis. FASEB J. 29, 3054-3064.

Huang J., Liu L., Feng M., An S., Zhou M., Li Z., Qi J. and Shen H. (2015a). Effect of $CoCl_2$ on fracture repair in a rat model of bone fracture. Mol. Med. Rep. 12, 5951-5956.

Huang Y., Zheng Y., Jia L. and Li W. (2015b). Long noncoding RNA H19 promotes osteoblast differentiation via TGF-β1/Smad3/HDAC signaling pathway by deriving miR-675. Stem Cells 33, 3481-3492.

Huang J., Peng J., Cao G., Lu S., Liu L., Li Z., Zhou M., Feng M. and Shen H. (2016). Hypoxia-induced microRNA-429 promotes differentiation of MC3T3-E1 osteoblastic cells by mediating ZFPM2 expression. Cell. Physiol. Biochem. 39, 1177-1186.

Huarte M. (2015). The emerging role of lncRNAs in cancer. Nat. Med. 21, 1253-1261.

Jiang C., Sun J., Dai Y., Cao P., Zhang L., Peng S., Zhou Y., Li G., Tang J. and Xiang J. (2015). HIF-1A and C/EBPs transcriptionally regulate adipogenic differentiation of bone marrow-derived MSCs in hypoxia. Stem Cell Res. Ther. 6, 21.

Kolling M., Genschel C., Kaucsar T., Hubner A., Rong S., Schmitt R., Sorensen-Zender I., Haddad G., Kistler A., Seeger H., Kielstein J.T., Fliser D., Haller H., Wuthrich R., Zornig M., Thum T. and Lorenzen J. (2018). Hypoxia-induced long non-coding RNA Malat1 is dispensable for renal ischemia/reperfusion-injury. Sci. Rep. 8, 3438.

Kurebayashi S., Sumitani S., Kasayama S., Jetten A.M. and Hirose T. (2001). TNF-alpha inhibits 3T3-L1 adipocyte differentiation without downregulating the expression of C/EBPbeta and delta. Endocr. J 48, 249-253.

Li T., Hu J., Gao F., Du X., Chen Y. and Wu Q. (2017). Transcription factors regulate GPR91-mediated expression of VEGF in hypoxia-induced retinopathy. Sci. Rep. 7, 45807.

Li X., Zhao J., Zhang H. and Cai J. (2020). Silencing of lncRNA metastasis-associated lung adenocarcinoma transcript 1 inhibits the proliferation and promotes the apoptosis of gastric cancer cells through regulating microRNA-22-3p-mediated ErbB3. Onco Targets Ther. 13, 559-571.

Liu Y., Guo G., Zhong Z., Sun L., Liao L., Wang X., Cao Q. and Chen H. (2019a). Long non-coding RNA FLVCR1-AS1 sponges miR-155 to promote the tumorigenesis of gastric cancer by targeting c-Myc. Am. J. Transl. Res. 11, 793-805.

Liu K.S., Pan F., Mao X.D., Liu C. and Chen Y.J. (2019b). Biological functions of circular RNAs and their roles in occurrence of reproduction and gynecological diseases. Am. J. Transl. Res. 11, 1-15.

Liu H., Shi C. and Deng Y. (2020). MALAT1 affects hypoxia-induced vascular endothelial cell injury and autophagy by regulating miR-19b-3p/HIF-1α axis. Mol. Cell. Biochem. 466, 25-34.

Livak K.J. and Schmittgen T.D. (2001). Analysis of relative gene expression data using real-time quantitative PCR and the 2(-Delta Delta C(T)) Method. Methods 25, 402-408.

Maes C., Carmeliet G. and Schipani E. (2012). Hypoxia-driven pathways in bone development, regeneration and disease. Nat. Rev. Rheumatol. 8, 358-366.

Maes C., Coenegrachts L., Stockmans I., Daci E., Luttun A., Petryk A., Gopalakrishnan R., Moermans K., Smets N., Verfaillie C.M., Carmeliet P., Bouillon R. and Carmeliet G. (2006). Placental growth factor mediates mesenchymal cell development, cartilage turnover, and bone remodeling during fracture repair. J. Clin. Invest. 116, 1230-1242.

Michalik K.M., You X., Manavski Y., Doddaballapur A., Zornig M., Braun T., John D., Ponomareva Y., Chen W., Uchida S., Boon R.A. and Dimmeler S. (2014). Long noncoding RNA MALAT1 regulates endothelial cell function and vessel growth. Circ. Res. 114, 1389-1397.

Peng S., Cao L., He S., Zhong Y., Ma H., Zhang Y. and Shuai C. (2018). An overview of long noncoding RNAs involved in bone regeneration from mesenchymal stem cells. Stem Cells Int. 2018, 8273648.

Potente M., Gerhardt H. and Carmeliet P. (2011). Basic and therapeutic aspects of angiogenesis. Cell 146, 873-887.

Singpiel A., Kramer J., Maus R., Stolper J., Bittersohl L.F., Gauldie J., Kolb M., Welte T., Sparwasser T. and Maus U.A. (2018). Adenoviral vector-mediated GM-CSF gene transfer improves anti-mycobacterial immunity in mice - role of regulatory T cells. Immunobiology 223, 331-341.

Voellenkle C., Garcia-Manteiga J.M., Pedrotti S., Perfetti A., De Toma I., Da S.D., Maimone B., Greco S., Fasanaro P., Creo P., Zaccagnini G., Gaetano C. and Martelli F. (2016). Implication of Long noncoding RNAs in the endothelial cell response to hypoxia revealed by RNA-sequencing. Sci. Rep. 6, 24141.

Wang C., Qu Y., Suo R. and Zhu Y. (2019). Long non-coding RNA MALAT1 regulates angiogenesis following oxygen-glucose deprivation/reoxygenation. J. Cell. Mol. Med. 23, 2970-2983.

Xiao X., Zhou T., Guo S., Guo C., Zhang Q., Dong N. and Wang Y. (2017). LncRNA MALAT1 sponges miR-204 to promote osteoblast differentiation of human aortic valve interstitial cells through up-regulating Smad4. Int. J. Cardiol. 243, 404-412.

Xie H., Liao X., Chen Z., Fang Y., He A., Zhong Y., Gao Q., Xiao H., Li J., Huang W. and Liu Y. (2017). LncRNA MALAT1 inhibits apoptosis and promotes invasion by antagonizing miR-125b in bladder cancer cells. J. Cancer 8, 3803-3811.

Xiong Z., Wang L., Wang Q. and Yuan Y. (2018). LncRNA MALAT1/miR-129 axis promotes glioma tumorigenesis by targeting SOX2. J. Cell. Mol. Med. 22, 3929-3940.

Zhu L. and Xu P.C. (2013). Downregulated LncRNA-ANCR promotes osteoblast differentiation by targeting EZH2 and regulating Runx2 expression. Biochem. Biophys. Res. Commun.432, 612-617.

Accepted December 5, 2022